SUPPORTING INFORMATION for

Influences of El Niño–Southern Oscillation on summertime ozone pollution over central-eastern China during 1950–2014

Yuexuanzi Wang [1], Yingying Yan [1*], Jintai Lin [2], Shaofei Kong [1, 3], Aili Song [1], Jing Ma [1]

[1] Department of Atmospheric Science, School of Environmental Sciences, China University of Geosciences, Wuhan, 430074, China

[2] Laboratory for Climate and Ocean-Atmosphere Studies, Department of Atmospheric and Oceanic Sciences, School of Physics, Peking University, Beijing 100871, China

[3] Department of Environmental Science and Engineering, School of Environmental Studies, China University of Geosciences, Wuhan, 430074, China

Correspondence to: Yingying Yan (yanyingying@cug.edu.cn)

S1. The statistical model of Kolmogorov-Zurbenko (KZ) filter

In our previous study (Wang et al., 2021), We use the Kolmogorov-Zurbenko (KZ) filter model to separate the influences of meteorology and emission-related trends.

$$X_{LT}(t) = X_{LT}^{EMI}(t) + X_{LT}^{MET}(t)$$

Where X_{LT} means the long-term component, X_{LT}^{EMI} means emission-related long-term components, and X_{LT}^{MET} means meteorology-related long-term series. The slope of the linear regression between time series and components represent the linear trends (Seo et al., 2018). The factors we considered include surface air temperature, surface relative humidity, sea level pressure, horizontal wind fields and daily precipitation.

The KZ filter's results show that the surface ozone long-term trend is mainly contributed by anthropogenic emissions, while there is little trend in time series of meteorological-contributed ozone. Therefore, we use the long-term trend of ozone to represent the emission-attributed trend in this study.

Seo, J., Park, D.-S. R., Kim, J. Y., Youn, D., Lim, Y. B., and Kim, Y.: Effects of meteorology and emissions on urban air quality: a quantitative statistical approach to long-term records (1999–2016) in Seoul, South Korea. Atmospheric Chemistry and Physics, 18(21), 16121–16137. https://doi.org/10.5194/acp-18-16121-2018, 2018.

Wang, Y., Yan, Y., Duan, K., Kong, S., Lin, J., Zheng, H., Song, A., and Zhang, Z.: Effect of springtime thermal forcing over Tibetan Plateau on summertime ozone in Central China during the period 1950-2019, Atmospheric Research, 261, 10.1016/j.atmosres.2021.105735, 2021.

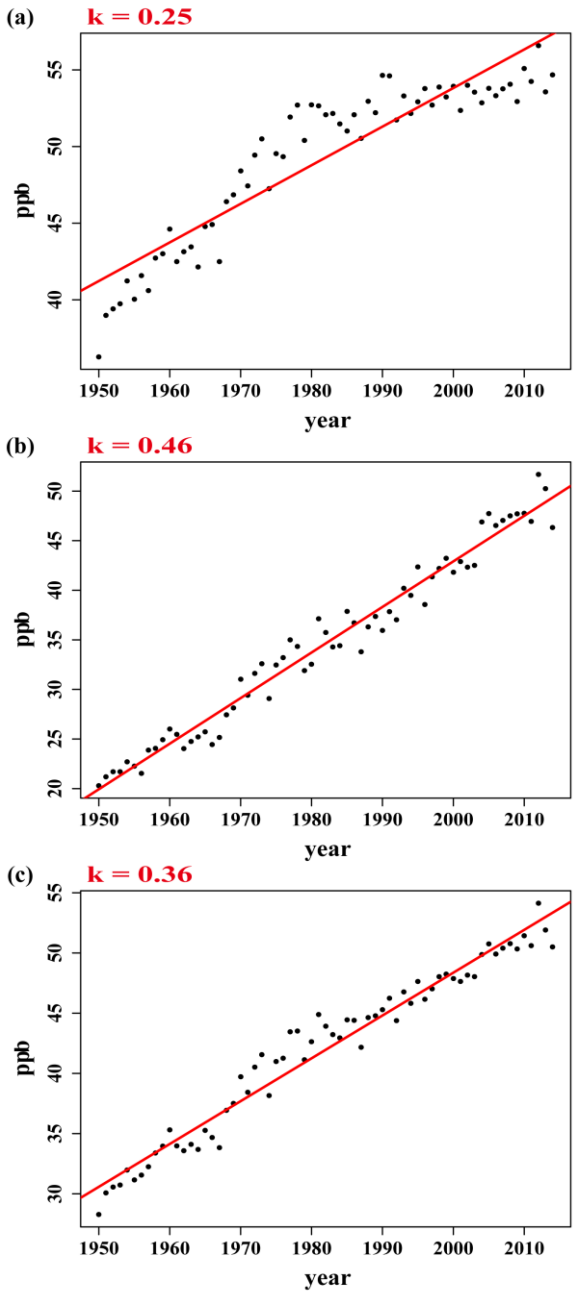

Figure S1. The emission-related trends are (a) 0.25 ppb yr^{-1}, (b) 0.46 ppb yr^{-1} and (c) 0.36 ppb yr^{-1} over the north part, south part and the whole central-eastern China, respectively, during 1950–2014 calculated by CMIP6 simulations.

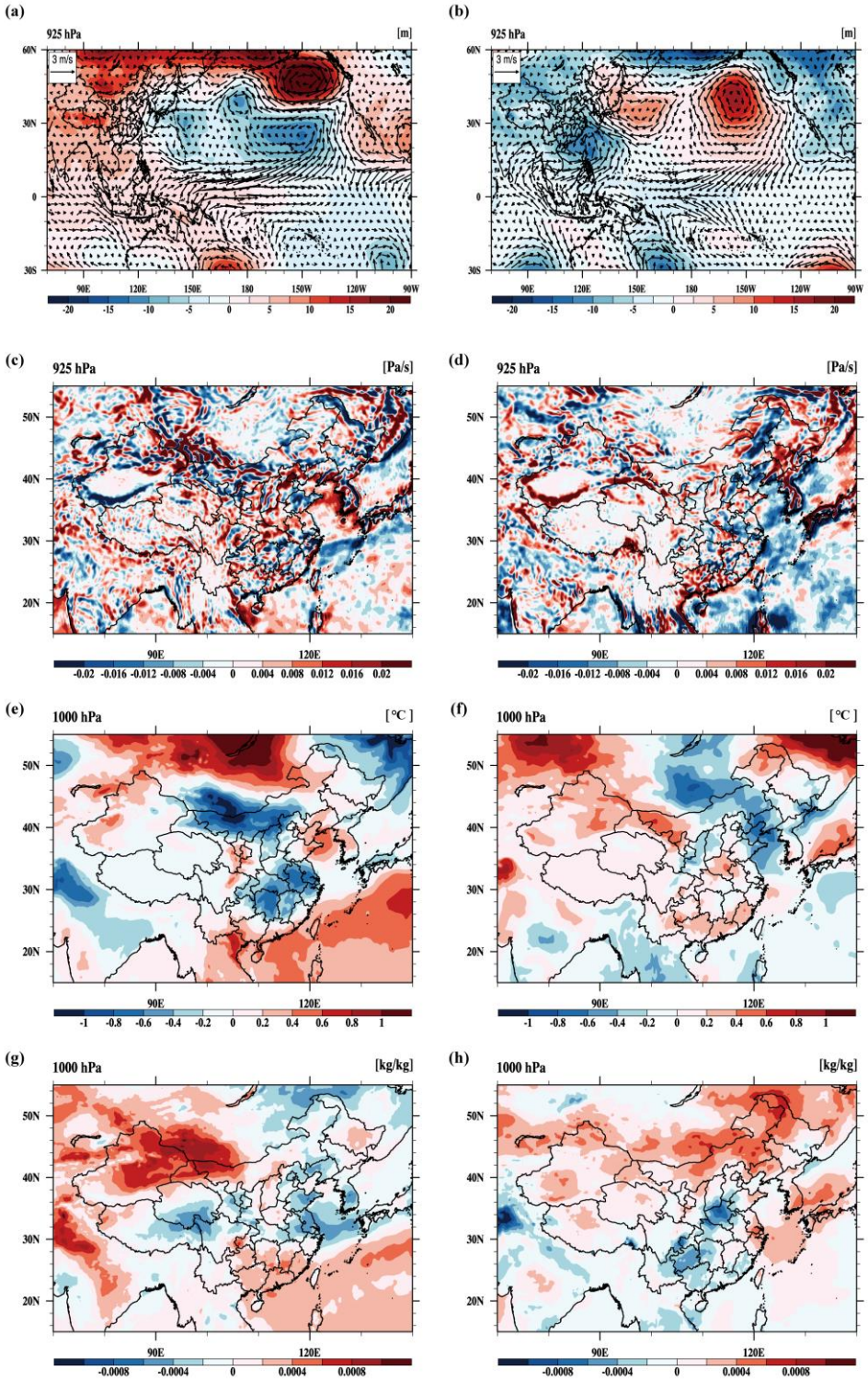

Figure S2. The anomalies of ERA5 summertime horizontal wind fields and geopotential height, vertical velocity, surface air temperature and specific humidity averaged over the study period (2005–2017) and the El Niño (a/c/e/g) and La Niña (b/d/f/h) years.

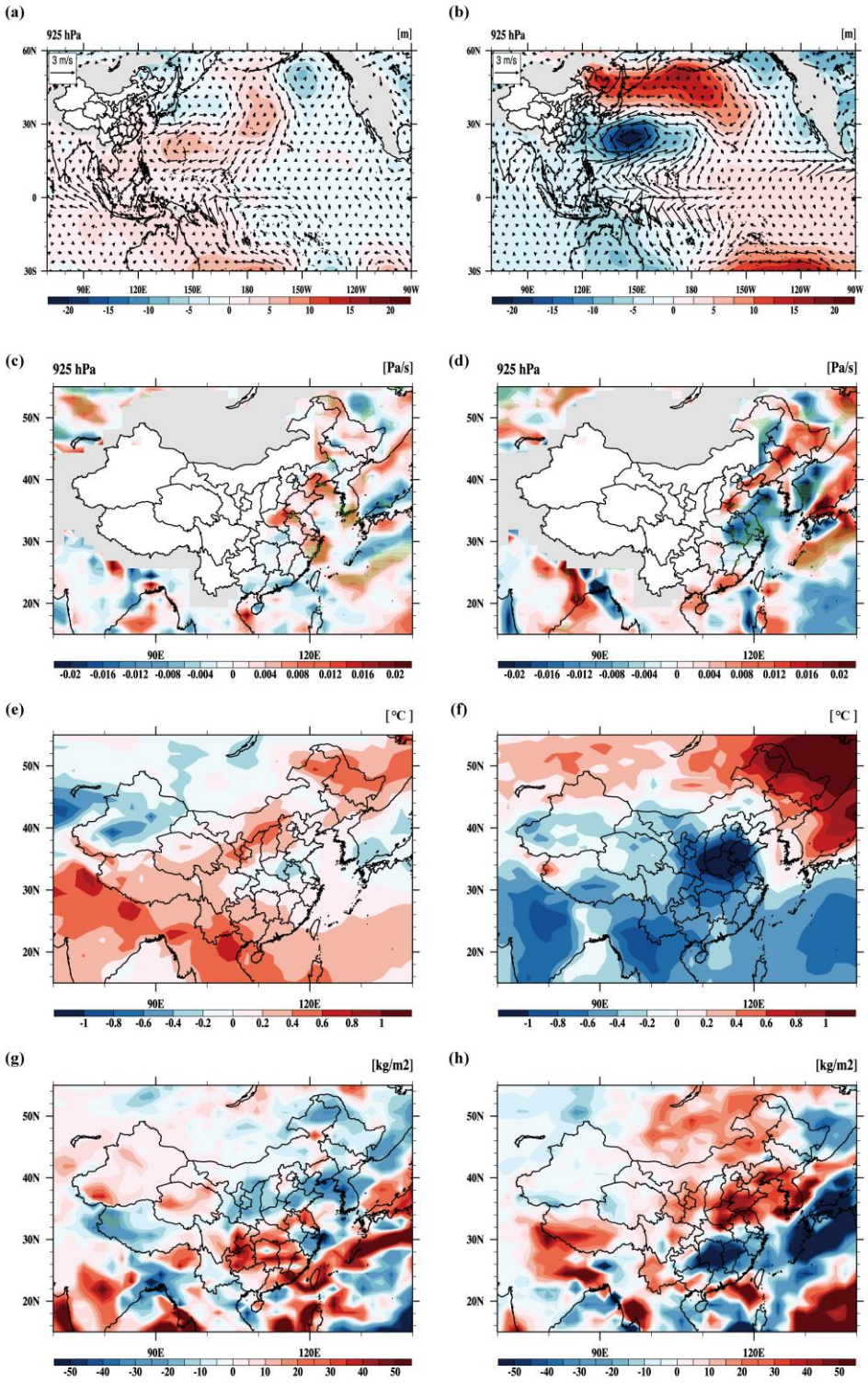

Figure S3. The anomalies of CMIP6 summertime horizontal wind fields and geopotential height, vertical velocity, surface air temperature and precipitation averaged over the study period (1950–2014) and the El Niño (a/c/e/g) and La Niña (b/d/f/h) years.

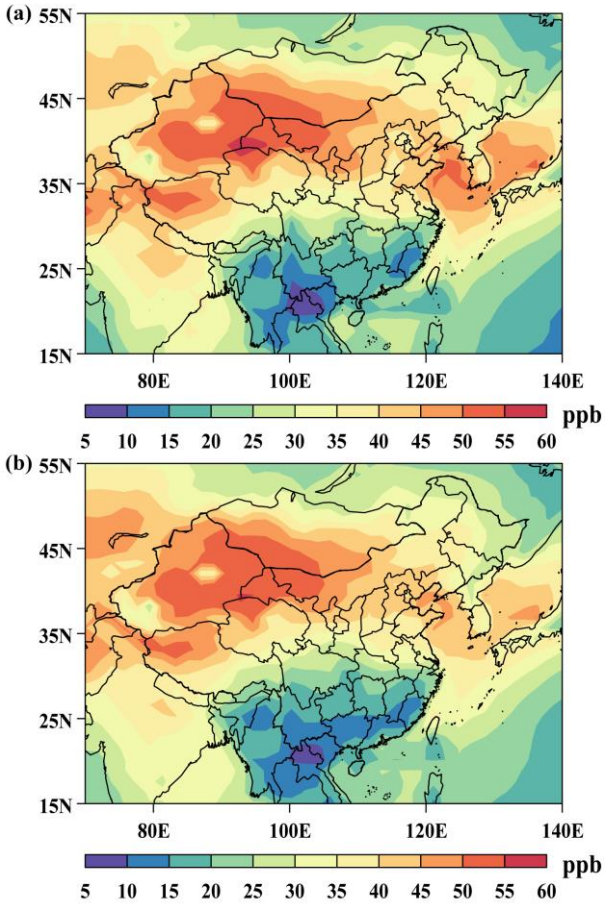

Figure S4. Spatial distribution of detrended summertime surface ozone concentrations during El Niño (a) and La Niña (b) years.

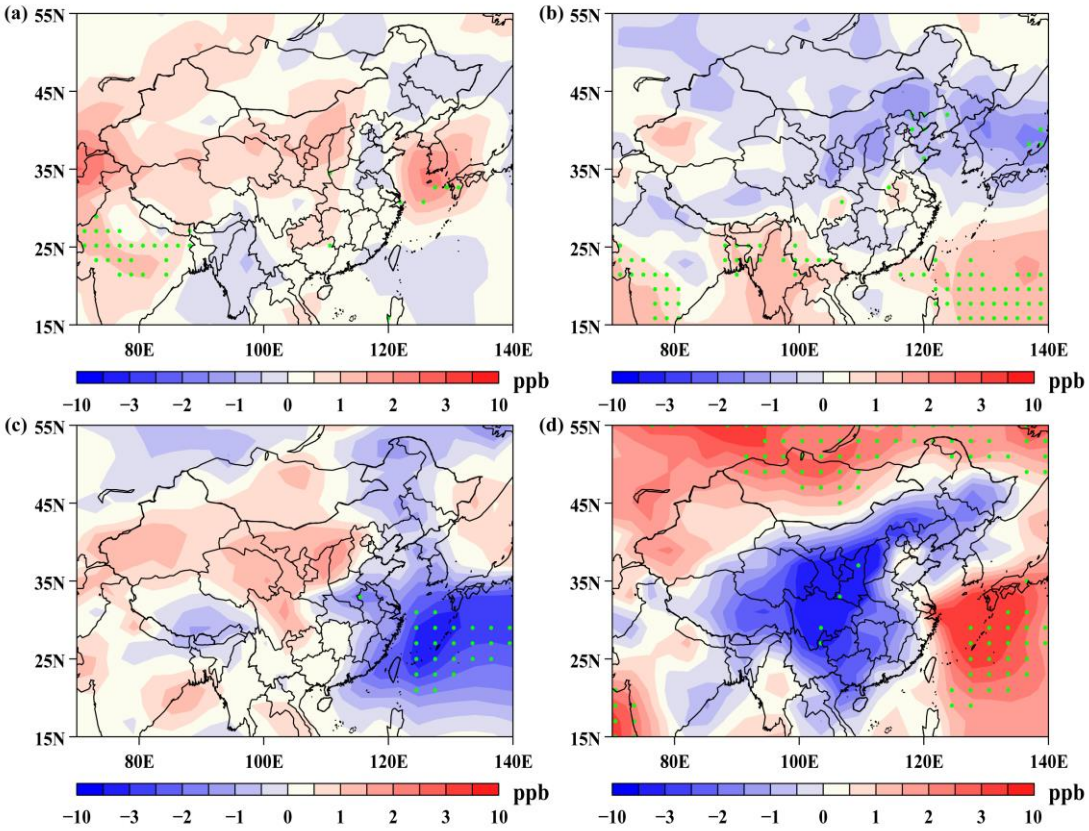

Figure S5. The summertime surface ozone anomalies in El Niño (a/c) and La Niña (b/d) events calculated based on MPI-ESM-1-2-HAM/EC-Earth3-AerChem data. The green dots indicate the P-value < 0.1.

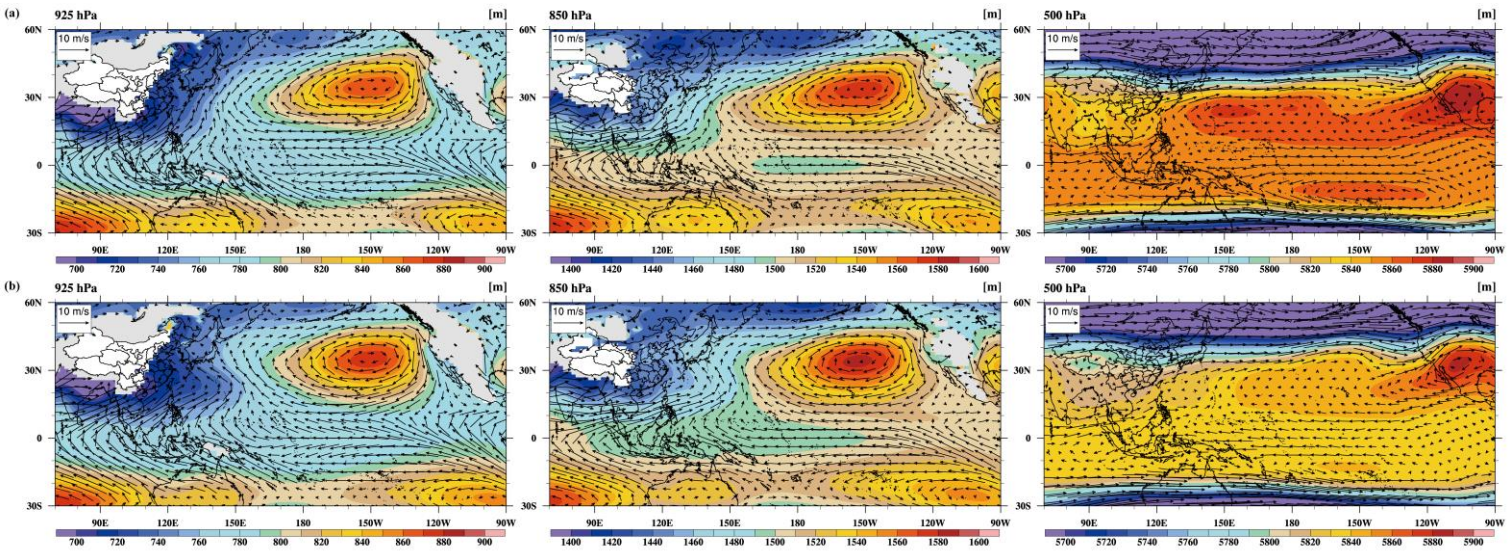

Figure S6. Spatial distributions of summertime horizontal wind fields and geopotential height at 925 hPa, 850 hPa and 500 hPa during El Niño (a) and La Niña (b) years. The missing values shown in grey areas are not provided by CMIP6 simulations because of the topographic.

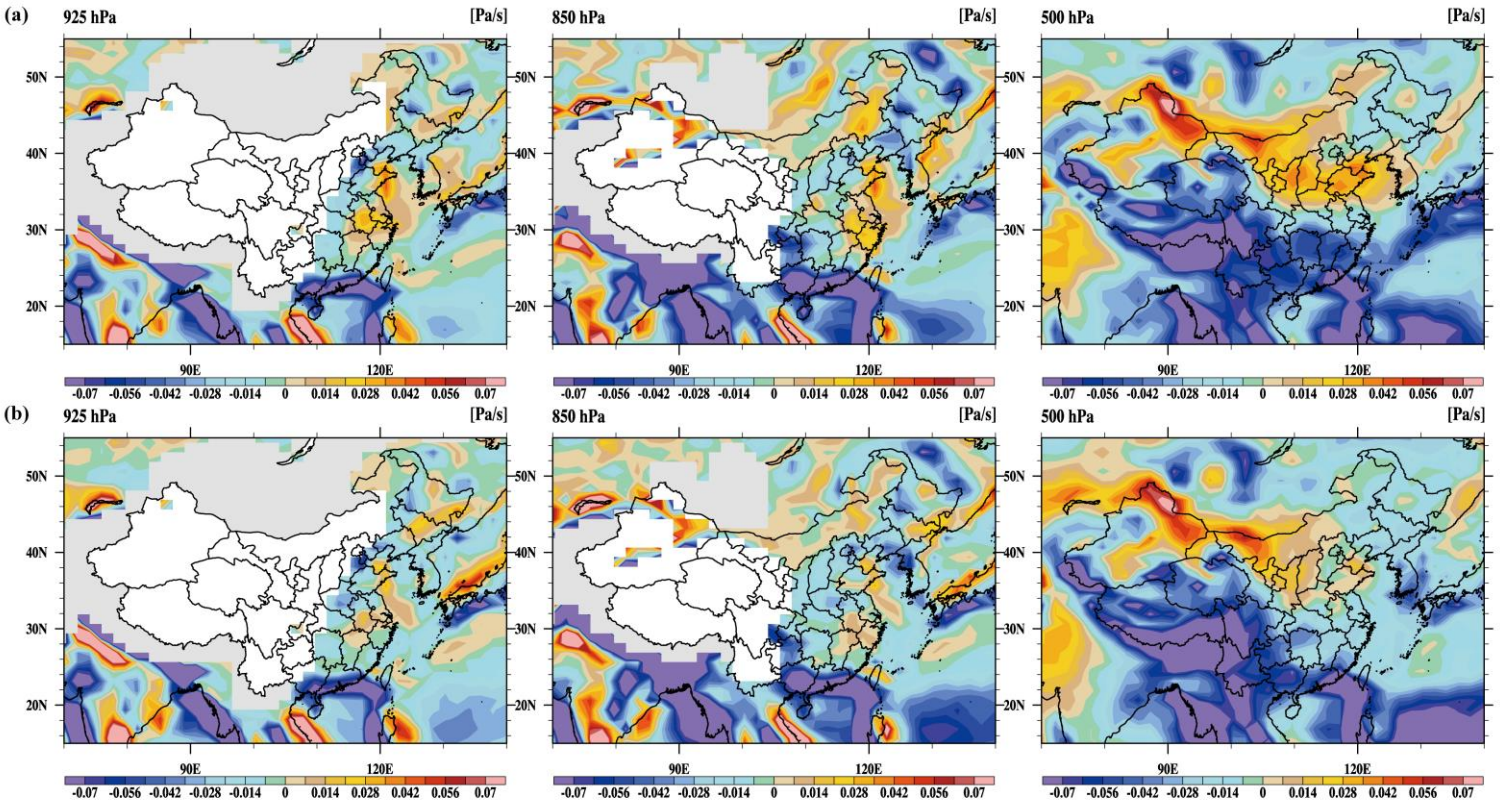

Figure S7. Spatial distributions of summertime vertical velocity at 925 hPa, 850 hPa and 500 hPa during El Niño (a) and La Niña (b) years. The missing values shown in grey areas are not provided by CMIP6 simulations because of the topographic.

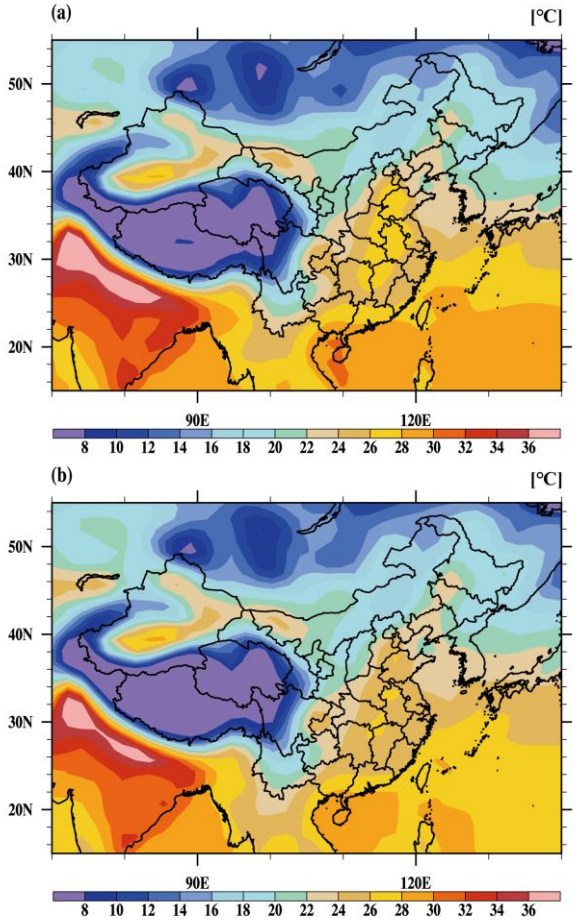

Figure S8. Spatial distribution of summertime surface air temperature during El Niño (a) and La Niña (b) years.

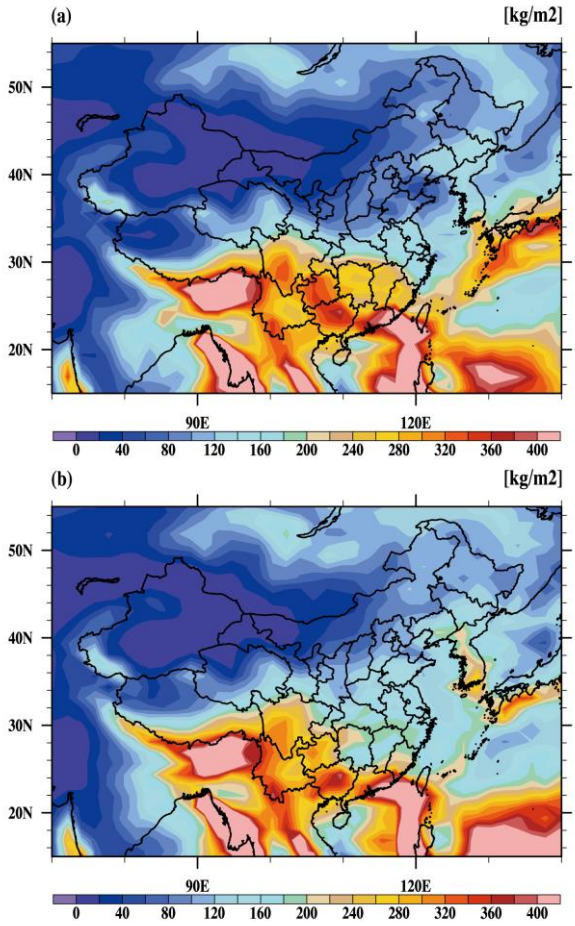

Figure S9. Spatial distribution of summertime precipitation during El Niño (a) and La Niña (b) years.